

# Study on the phase structures and toughening mechanism in PP/EPDM/SiO<sub>2</sub> ternary composites

Hong Yang, Qin Zhang, Min Guo, Cong Wang, Rongni Du, Qiang Fu \*

State Key Laboratory of Polymer Materials Engineering, Department of Polymer Science and Materials, Sichuan University, Chengdu 610065, China

Received 7 September 2005; received in revised form 17 January 2006; accepted 22 January 2006

Available online 8 February 2006

## Abstract

In this paper, EPDM rubber and nano-SiO<sub>2</sub> particles were employed to modify PP simultaneously. Our goal was to control the distribution and dispersion of EPDM and nano-SiO<sub>2</sub> particles in PP matrix by using an appropriate processing method and adjusting the wettability of nano-SiO<sub>2</sub> particles toward PP and EPDM, so as to achieve a simultaneous enhancement of toughness and modulus of PP. With regard to this, two kinds of nano-SiO<sub>2</sub> particles (with hydrophilic or hydrophobic) as well as two processing methods (one-step or two-step) were employed to prepare PP/EPDM/SiO<sub>2</sub> ternary composites. A unique structure with the majority of EPDM particles surrounded by SiO<sub>2</sub> particles was first observed by using hydrophilic SiO<sub>2</sub> and two-step processing method, resulting in a dramatic increase of Izod impact strength as the rubber content in the range of brittle–ductile transition (15–20 wt%). The observation that poor adhesion and poor compatibility between particles and PP matrix could result in a significant increase in Izod impact strength was unusual and needed further investigation. This could be tentatively understood as a consequence of the overlap of the ‘stress volume’ between EPDM and SiO<sub>2</sub> particles due to the formation of the unique structure. Our work provided a deep understanding of the toughening mechanism and a new way for the preparation of high performance polymer composites.

© 2006 Elsevier Ltd. All rights reserved.

**Keywords:** PP/EPDM/nano-SiO<sub>2</sub> ternary composites; Phase structures; Toughening mechanism

## 1. Introduction

Polymer blending or compounding receives increasingly interest because it is a relatively easy way to obtain new materials with balanced properties. Generally, elastomer is used to improve the toughness but sacrifices the modulus of polymers. Adding inorganic filler can enhance the stiffness but result in a decrease of toughness. To overcome the drawback resulted by only adding elastomer or filler, a lot of work has been done on polymer/elastomer/filler ternary system, where both elastomer and filler were used to enhance the toughness and stiffness simultaneously [1–11]. To achieve the best combination of mechanical properties, the key is to control the dispersion and phase morphology of ternary composites. Concerning the phase morphology containing both elastomer and filler dispersed in polymer matrix, separated microstructure where the elastomer and filler are dispersed in polymer matrix separately, and core–shell microstructure with the filler

covered the elastomer, are the two morphologies commonly observed in ternary composites. Argument exists on whether separated dispersion or core–shell microstructure is favor to toughening. Matonis etc. [1,2] concluded that core–shell structure helps increase the toughness, and the thinner the elastomer and the stronger the adhesion between filler and matrix, the higher the toughness of the composites. However, Jancar etc. [11] has shown that the modulus is increased in a condition of separated dispersion while the core–shell microstructure can improve the toughness. The mechanical properties and the morphologies of ternary blends of polycarbonate with a mechacrylated butadiene–styrene impact modifier and various brittle polymers were investigated by Paul et al. They found, very interestingly, that for a better toughness the modifier should be located in the brittle polymer in ternary blend [12]. There are several factors, such as composition, processing conditions, adhesion between filler and elastomer, which may affect the dispersion and microstructure [3–10]. Most work is qualitative on toughening mechanism while the quantitative relationship between morphology and property has not been established yet so far.

Polypropylene (PP) is one of the important commodity polymers. It is widely used in automobile, household appliance and construction industry due to its balanced mechanical

\* Corresponding author. Tel.: +86 28 854 609 53; fax: +86 28 854 054 02.  
E-mail address: [qiangfu@scu.edu.cn](mailto:qiangfu@scu.edu.cn) (Q. Fu).

properties. The application of PP, however, is limited by its brittleness, especially at low temperature, as well as low stiffness at elevated temperature. In order to improve the impact toughness of PP and extend its application range, a lot of extensive and thorough researches on PP toughened with different particles (including both rubber and rigid particles) have been made. Concerning the toughening mechanism, over the years various conceptual models, including crazing, cavitations and shear yielding, have been proposed and worked out [13–21]. One of the most important findings in polymer-toughening is known as the critical matrix ligament thickness ( $\tau_c$ ) theory, which is developed by Wu after an investigation on nylon 6/EPDM blends [22–25] and extended by Qi after an investigation on PP/EPDM blends [26,27]. Only when the matrix ligament thickness ( $\tau$ ) is smaller than  $\tau_c$  could the shear yielding of matrix ligament exist and does a sharp brittle–ductile transition (B–D transition) of blends occur. More than 10 times' increase in impact strength is observed for PP/EPDM blends at the B–D transition. The key is that the stress fields around individual particle must interfere or overlap with each other and pervade within the matrix to realize a massive shear yielding. A percolation process of stress volume spheres has been successfully used to explain the phenomenon of the B–D transition [28–30].

In this paper, EPDM and nano-SiO<sub>2</sub> particles will be employed to modify PP simultaneously. Our goal is to control the dispersion and distribution of EPDM and nano-SiO<sub>2</sub> particles in PP matrix by using an appropriate processing method and adjusting the wettability of SiO<sub>2</sub> particles toward PP and EPDM, so that the stress fields around EPDM nano-SiO<sub>2</sub> particle can interfere or overlap in PP matrix. In this way, part of EPDM can be replaced by nano-SiO<sub>2</sub> particles for toughening, thus a simultaneous enhancement of toughness and modulus can be achieved. Therefore, two kinds of nano-SiO<sub>2</sub> particles (with hydrophilic or hydrophobic) and two processing methods (one-step or two-step) will be used to prepare PP/EPDM/SiO<sub>2</sub> ternary composites. The relationships between phase structure and impact strength of PP/EPDM/SiO<sub>2</sub> composites are discussed in detail.

## 2. Experimental

### 2.1. Materials

The materials used for the preparation of PP/EPDM/SiO<sub>2</sub> composites are listed in Table 1. Polypropylene (PP), EPDM and fumed nano-SiO<sub>2</sub> particles used in our study were commercially available. The hydrophobic nano-SiO<sub>2</sub>(A-SiO<sub>2</sub>)

was treated by coupling agent D4 (octamethyl cyclotetrasiloxane) before used while the hydrophilic nano-SiO<sub>2</sub>(B-SiO<sub>2</sub>) was received without any pretreatment.

### 2.2. Sample preparation

Two processing methods were employed to prepare PP/elastomer/filler ternary composites. One was called one-step processing method, in which the elastomer and the filler were directly melt-blended with PP matrix. Another one was called two-step processing method, in which the elastomer and the filler were mixed by means of a two-roll mill at room temperature for 10 min to get masterbatch first, and then the masterbatch was melt blended with pure PP. The blending was conducted in a two-screw extruder at 140–210 °C, and then injection molded in PS40E5ASE (Japan) at 180–210 °C to obtain standard specimen for mechanical properties tests.

### 2.3. Mechanical tests

#### 2.3.1. Izod impact strength test

The notched Izod impact strength was used to evaluate the toughness of samples. The notched specimens were tested with a VJ-40 impact test machine at room temperature, according to GB/T 1834-1996 standard. Each impact test was repeated at least five times, and the results were averaged.

#### 2.3.2. Yield tensile strength, flexural strength and modulus test

Standard tensile tests were conducted on dumbbell shaped specimens using an AG-10TA tensile testing machine at room temperature. Test speed was kept at 50 mm/min, according to GB/T 1040-92 standard. The flexural strength and flexural modulus were measured using an AG-10TA flexural testing machine with a speed of 2 mm/min according to GB 9341-88 standard. Both of these tests were carried out in five folds.

### 2.4. Scanning electron microscopy (SEM) experiments

The morphology of the blends was studied by preferential etching of EPDM phase in dimethylbenzene for 2 h. The samples were cryogenically fractured in the direction perpendicular to flow direction in liquid nitrogen before etching. The etched samples were carefully washed for several times by using fresh dimethylbenzene, then alcohol washed for three times. The samples were dried under vacuum at room temperature for 24 h. Then the fractured samples were observed in a JEOL JSM-5900LV SEM instrument, using an

Table 1  
Materials

	Materials	Brand	Supplier	Characteristics
	PP	T30 s	Du Shan Zi Petroleum Chemical, China	MFI=2.64 g/10 min (230 °C, 2.16 kg)
	EPDM	EP35	Japan Synthetic Rubber Co. Ltd	PP content: 43% Mooney viscosity: 83(100 °C) the third monomer: ENB
Fumed nano-SiO <sub>2</sub>	Hydrophobic SiO <sub>2</sub> (A-SiO <sub>2</sub> )	JT-SQ	Chendu Today chemical Co. Ltd	Particle size: 10–30 nm $S_{(BET)}=200 \text{ m}^2/\text{g}$
	Hydrophilic SiO <sub>2</sub> (B-SiO <sub>2</sub> )	HL-150	Guangzhou GBS High Tech & Industry Co.	Particle size: 15–20 nm $S_{(BET)}=150 \pm 10 \text{ m}^2/\text{g}$

acceleration voltage of 20 kV, which could show the dispersion of elastomer and filler in PP matrix.

### 3. Results and discussions

To better understand the properties and morphologies of the ternary blends, we begin with PP/A-SiO<sub>2</sub>, PP/B-SiO<sub>2</sub> and PP/EPDM binary blends. For both PP/A-SiO<sub>2</sub> and PP/B-SiO<sub>2</sub> binary blends, the Izod impact strength decreases with the addition of SiO<sub>2</sub> particles while the tensile strength, flexural strength and flexural modulus slightly increase with the SiO<sub>2</sub> content as shown in Fig. 1(a)–(d). For PP/EPDM binary blend, as expected, Izod impact strength increases dramatically and a sharp brittle–ductile transition is achieved when rubber content reaches a certain value, accompanied with a decrease of the tensile strength, flexural strength and flexural modulus, as shown in Fig. 2(a)–(d). It can be seen that a sharp brittle–ductile transition occurs at 15–20 wt% of EPDM content. The toughness of PP/EPDM blend becomes independent of EPDM content when EPDM content is more than 30 wt%. However, when EPDM and nano-SiO<sub>2</sub> particles were used together, a simultaneous increase of the toughness and stiffness in PP/EPDM/SiO<sub>2</sub> ternary composites can be achieved by using

an appropriate processing method and adjusting the wettability of SiO<sub>2</sub> particles toward PP and EPDM. Fig. 3 shows the Izod impact strength of different PP/EPDM/SiO<sub>2</sub> composites prepared by two processing methods, respectively. Both hydrophobic SiO<sub>2</sub> particles (A-SiO<sub>2</sub>) and hydrophilic SiO<sub>2</sub> particles (B-SiO<sub>2</sub>) were used here. By using hydrophobic SiO<sub>2</sub> particles (A-SiO<sub>2</sub>), or by using hydrophilic SiO<sub>2</sub> particles (B-SiO<sub>2</sub>) but one-step processing method, one observes only a slight increase of Izod impact strength. By using hydrophilic SiO<sub>2</sub> particles (B-SiO<sub>2</sub>) and two-step processing method, however, a remarkable increase of Izod impact strength can be seen. A comparison of the stiffness between PP/EPDM/B-SiO<sub>2</sub> (80:20:5) ternary blend and PP/EPDM (70:30) binary blend is list in Table 2. One observes similar Izod impact strength but higher tensile strength, flexural strength and modulus in ternary system.

It is unusual that hydrophilic SiO<sub>2</sub> is better than hydrophobic SiO<sub>2</sub> as a toughening agent based on the wettability of SiO<sub>2</sub> particles toward PP and EPDM. In other words, one in general does not expect hydrophilic filler mixed in hydrophobic polymer to produce materials with good properties. Therefore, SEM experiment was carried out to understand the phase morphology of PP/EPDM/SiO<sub>2</sub>

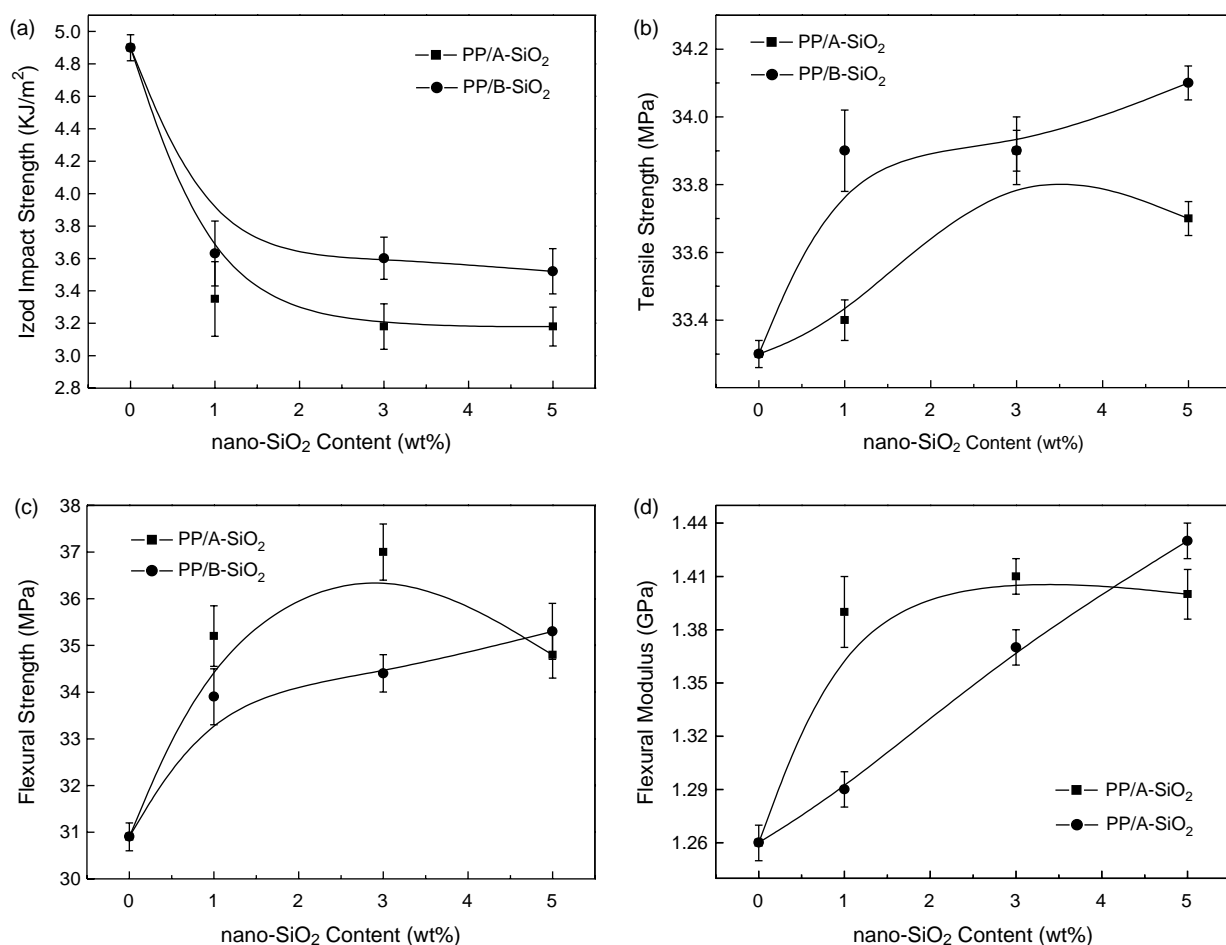


Fig. 1. Mechanical properties of PP/A-SiO<sub>2</sub> and PP/B-SiO<sub>2</sub> binary blends via nano-SiO<sub>2</sub> content (a) Izod impact strength; (b) tensile strength; (c) flexural strength; (d) flexural modulus.

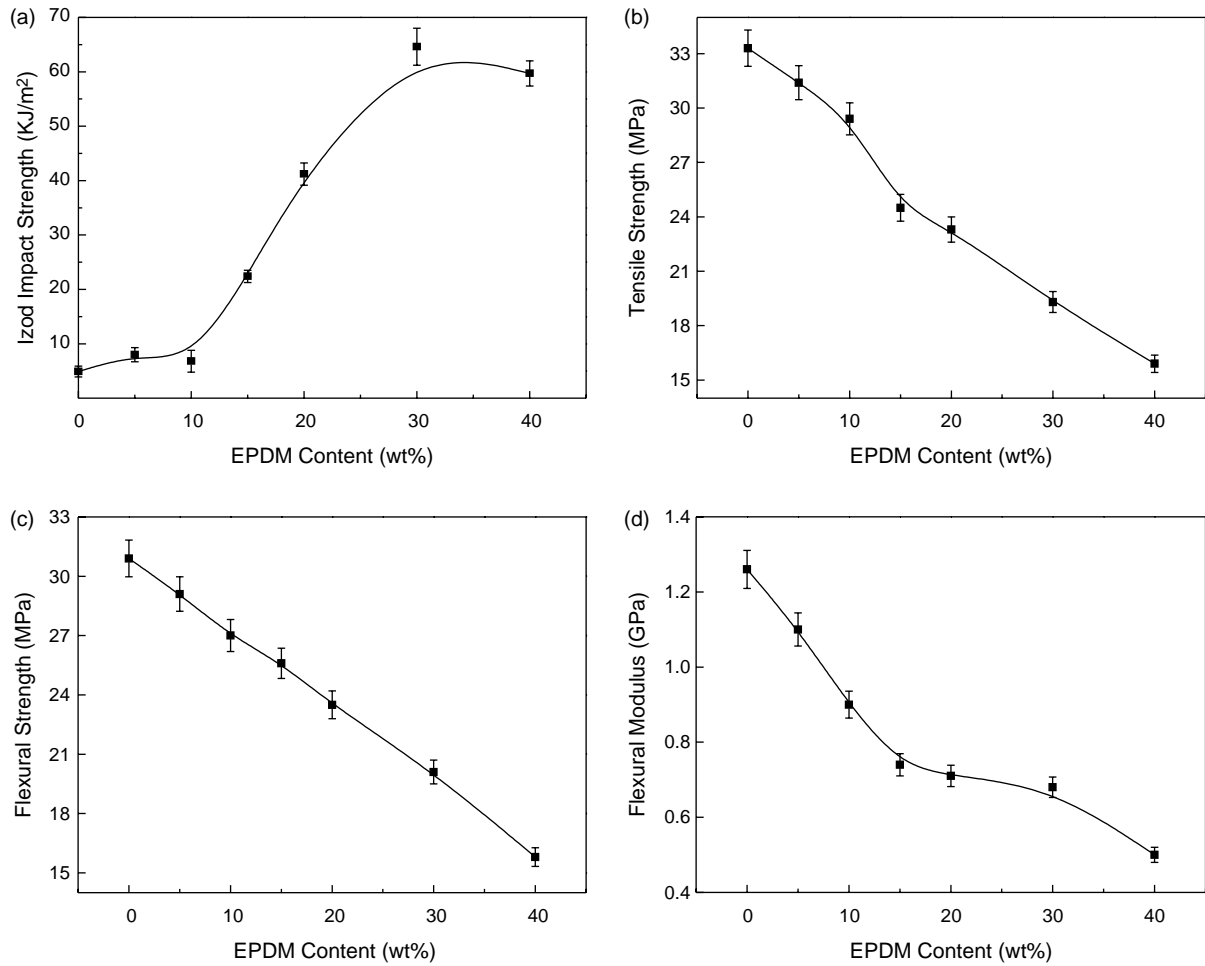


Fig. 2. Mechanical properties of PP/EPDM binary blend via EPDM content (a) Izod impact strength; (b) tensile strength; (c) flexural strength; (d) flexural modulus.

composites. Fig. 4 shows the phase morphology of the samples after selectively etching of EPDM rubber particles. For PP/EPDM/A-SiO<sub>2</sub> composites prepared by one-step processing method and two-step processing method, nearly no difference

of phase structure between them can be found. In these two cases, a core-shell structure is most likely formed since few A-SiO<sub>2</sub> particles (bright particles) can be seen in PP matrix (seen in Fig. 4(a) and (b)). For PP/EPDM/B-SiO<sub>2</sub> composites prepared by one-step processing method, large aggregates of B-SiO<sub>2</sub> particles with a size of 0.5–1.0 μm exist in PP matrix. As expected, there exists poor adhesion and poor compatibility between particles and PP matrix. Therefore, a separated dispersion structure with large B-SiO<sub>2</sub> aggregates is probably formed (seen in Fig. 4(c)). However, a unique phase structure that a large amount of B-SiO<sub>2</sub> particles agglomerate around EPDM particles (dark holes) and pervade over the PP matrix can be observed in PP/EPDM/B-SiO<sub>2</sub> composites prepared by

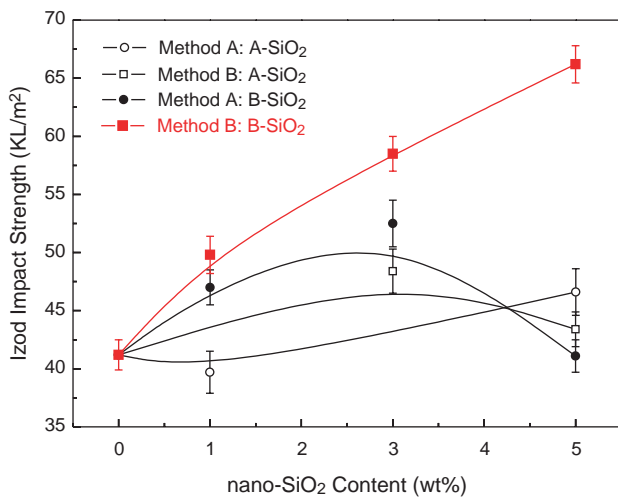


Fig. 3. Izod impact strength versus SiO<sub>2</sub> content for different PP/EPDM/SiO<sub>2</sub> composites prepared by two processing methods, respectively (PP/EPDM=80:20).

Table 2

The comparison of the mechanical properties between PP/EPDM/B-SiO<sub>2</sub> (80:20:5) prepared by two-step processing method and the pure PP/EPDM (70:30)

	Izod impact strength (kJ/m <sup>2</sup> )	Tensile strength (MPa)	Flexural strength (MPa)	Flexural modulus (GPa)
PP/EPDM/B-SiO <sub>2</sub> 80:20:5	66.2	21.9	23.6	0.83
PP/EPDM 70:30	64.6	19.3	20.1	0.68

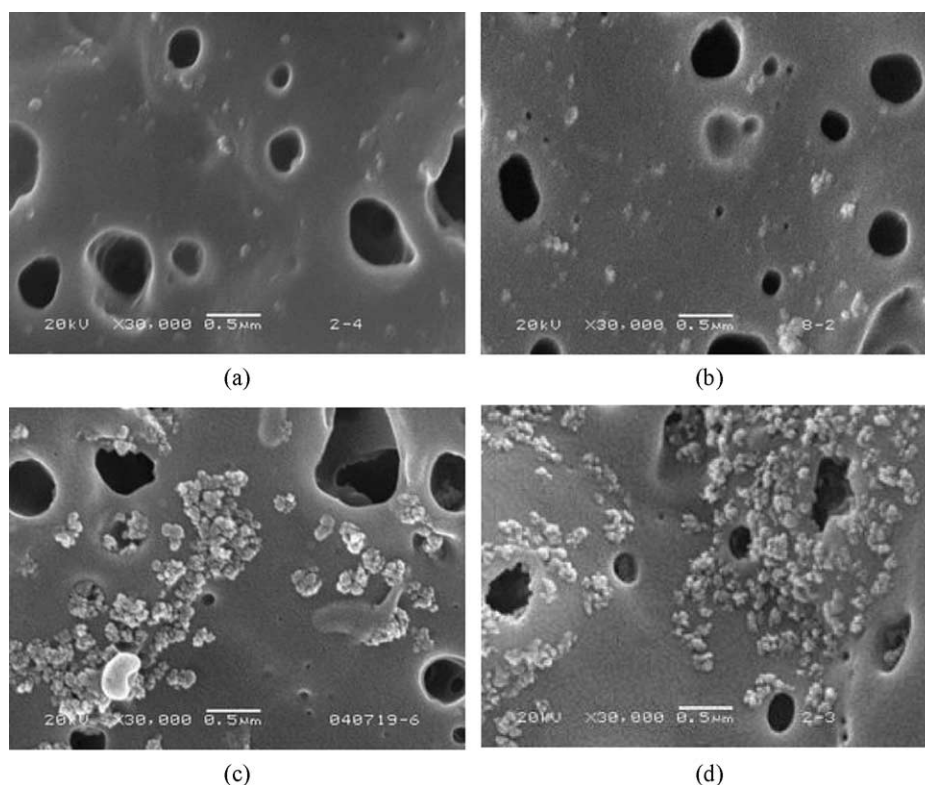


Fig. 4. SEM images of PP/EPDM/nano-SiO<sub>2</sub> (80:20:3) ternary composites (a) one-step, A-SiO<sub>2</sub>; (b) two-step, A-SiO<sub>2</sub>; (c) one-step, B-SiO<sub>2</sub>; (d) two-step, B-SiO<sub>2</sub>.

two-step processing method (seen in Fig. 4(d)). Though TEM experiment is needed to get more detailed information of the phase structure of these samples, it is reasonable to believe that it is a unique phase structure that is responsible for the improved Izod impact strength.

In order to provide evidence to the assertion that improved Izod impact strength of PP/EPDM/B-SiO<sub>2</sub> composites prepared by two-step processing method can be related to the formation of this unique phase structure, PP/EPDM/B-SiO<sub>2</sub> composites with three different rubber contents were studied. They were 10 wt% (brittle region), 20 wt% (brittle–ductile transition region) and 30 wt% (ductile region), respectively. The hydrophilic SiO<sub>2</sub> particles (B-SiO<sub>2</sub>) content varies from 1 to 5 wt%, and samples were all prepared by two-step processing method. Izod impact strength of PP/EPDM/B-SiO<sub>2</sub> composites as a function of B-SiO<sub>2</sub> content is shown in Fig. 5. It can be seen that, when EPDM content is 20 wt% (brittle–ductile transition region), the Izod impact strength of PP/EPDM/B-SiO<sub>2</sub> composites increases linearly with the increase of B-SiO<sub>2</sub> content. Specifically, the Izod impact strength increases from 41.2 to 66.2 kJ/m<sup>2</sup> as B-SiO<sub>2</sub> content varies from 0 to 5 wt%. In addition, the Izod impact strength of PP/EPDM (80:20) composite with 5 wt% B-SiO<sub>2</sub> particles content (66.2 kJ/m<sup>2</sup>) is almost the same as that of the pure PP/EPDM (70:30) composite (64.6 kJ/m<sup>2</sup>). The Izod impact strength of PP/EPDM/B-SiO<sub>2</sub> composites, however, increases slightly when EPDM content is 10 wt% (brittle region), and almost keeps constant when EPDM content is 30 wt% (ductile region).

Fig. 6 shows the phase structure of PP/EPDM/B-SiO<sub>2</sub> composites prepared by two-step processing method after selectively etching of EPDM rubber particles. The content of B-SiO<sub>2</sub> particles keeps at 3 wt%. Compared with Fig. 6(a)–(c), it can be found that the average size of EPDM particles (dark holes) almost keeps constant while the average interparticle distance decreases sharply with the increase of EPDM content, varying from 0.37 μm (10 wt% EPDM) to 0.08 μm (30 wt% EPDM). Obviously, the phase structure of PP/EPDM/B-SiO<sub>2</sub>

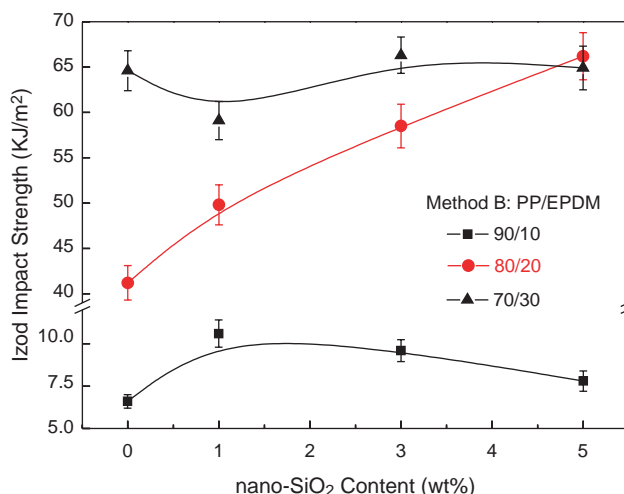


Fig. 5. Variation of Izod impact strength with B-SiO<sub>2</sub> content for various PP/EPDM composites.



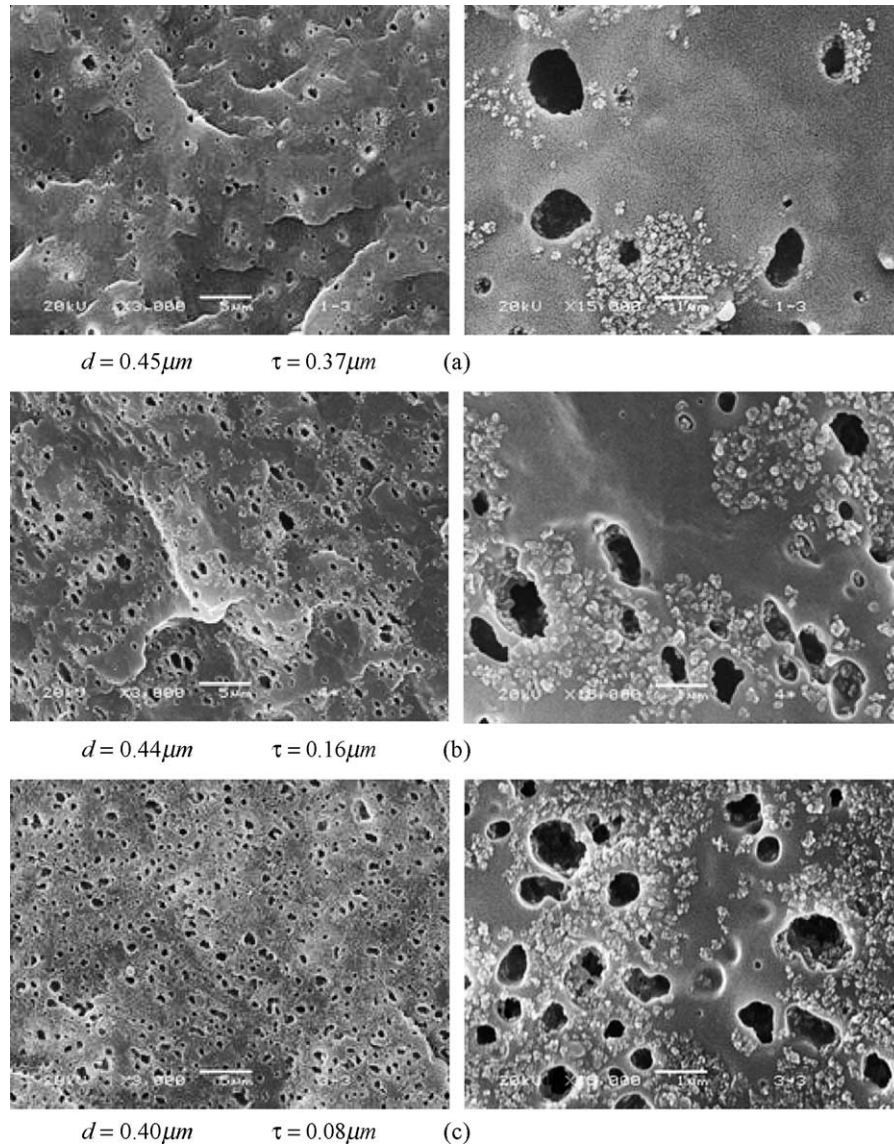


Fig. 6. SEM images of PP/EPDM/B-SiO<sub>2</sub> ternary composites prepared by two-step processing method (a) 90:10:3; (b) 80:20:3; (c) 70:30:3  $d$ , the average rubber particle diameter;  $\tau$ , the average interparticle distance.

composites varies with the EPDM content. For PP/EPDM/B-SiO<sub>2</sub> (90:10:3) composite, large interparticle distance (also called matrix–ligament thickness) is observed. Besides, some EPDM particles are surrounded by B-SiO<sub>2</sub> particles and a few B-SiO<sub>2</sub> particles can be seen in PP matrix. By adding 20 wt% of EPDM, however, the interparticle distance decreases sharply and a unique phase structure can be observed here, that is, a majority of EPDM particles are surrounded by B-SiO<sub>2</sub> particles, and meanwhile, a network of B-SiO<sub>2</sub> particles is developed and pervaded over the PP matrix. With the further addition of EPDM (30 wt%), not only are all EPDM particles surrounded by B-SiO<sub>2</sub> particles, but also do B-SiO<sub>2</sub> particles occupy the entire PP matrix. This finding is similar with what Paul had noted that for a better toughness the modifier should be located in the brittle polymer in ternary blend [12]. Here the modifier can be considered as EPDM particles and the brittle polymer as B-SiO<sub>2</sub> particles. Now it is logical to ask how this unique phase structure

forms via two-step processing method. The equilibrium morphology and the location of the filler within two-phase matrix formed by PP and EPDM, in principle, are determined by interfacial forces of thermodynamic origin and the wettability of SiO<sub>2</sub> particles toward PP and EPDM. In practice, an equilibrium distribution may not be achieved since kinetic issues could play a considerable role in some circumstances [12]. Due to its hydrophilic property, B-SiO<sub>2</sub> particles cannot be wetted by either PP or EPDM. Under the shear force, B-SiO<sub>2</sub> particles will be in this case effectively forced out from high viscosity of EPDM and will eventually agglomerate together in PP matrix just like in the case of one-step processing. Since the agglomerating process will take time, there exists an intermediate state where EPDM particles are surrounded by B-SiO<sub>2</sub> particles. This phase structure can be controlled and frozen in by solidification of PP via adjusting processing conditions including temperature and time.

### 3.1. Toughening mechanism

#### 3.1.1. Wu's theory

According to the framework of Wu's theory [22–25,28], for polymer/rubber binary composites, a sharp brittle–ductile transition occurred at a critical rubber particle size. And the critical particle size was related to the rubber volume fraction  $\phi_r$  by [23]:

$$\tau_c = d_c[(\pi/6\phi_r)^{1/3} - 1] \quad (1)$$

where  $d_c$  was the critical rubber particle diameter, and  $\tau_c$  the critical surface-to-surface interparticle distance, or the critical matrix–ligament thickness. The value of  $\tau_c$  was independent of the particle size and rubber volume fraction.  $\tau$  represented the average surface-to-surface interparticle distance (i.e. the average matrix–ligament thickness) and depended on the rubber volume fraction. If  $\tau < \tau_c$ , the continuum percolation of stress volume around rubber particles would occur; the matrix yielding would propagate and pervade over the entire matrix, and then the blend would be tough. On the contrary, if  $\tau > \tau_c$ , the matrix yielding could not propagate, and the blend failed in a brittle manner.

#### 3.1.2. Toughening mechanism

In this study, the hydrophilic SiO<sub>2</sub> particles tend to aggregate around the EPDM particles since hydrophilic SiO<sub>2</sub> particles can be wetted by neither PP nor EPDM. Showing as an example, the dispersion of hydrophilic SiO<sub>2</sub> particles in pure PP matrix is shown in Fig. 7. A poor wetting of the filler within the aggregates is seen (more clearly at high magnification, Fig. 7(b)). These poorly dispersed particles act as voids rather than stiff inclusion, resulting in a decrease of impact strength and only slightly increase of tensile strength, flexural strength and modulus, as can be observed in Fig. 1. For PP/EPDM/B-SiO<sub>2</sub> ternary composites, however, the two-step processing method is convenient to the dispersion of the B-SiO<sub>2</sub> particles and the formation of the unique structure that B-SiO<sub>2</sub> particles agglomerate around EPDM particles. These SiO<sub>2</sub>-surrounded EPDM particles can therefore be regarded as a soft core surrounded by rigid SiO<sub>2</sub> particles shell of comparable size, which could increase the effective size of the rubber particles. Then the stress fields around SiO<sub>2</sub> particle can interfere or

overlap with those around the EPDM particles when EPDM particles are closely surrounded by SiO<sub>2</sub> particles and a percolation of SiO<sub>2</sub> particles in PP matrix is formed. In this case, the stress fields around SiO<sub>2</sub> particles seem to serve as a bridge between two neighboring rubber particles. Therefore the overlap of the stress volume between EPDM and SiO<sub>2</sub> particles is believed to result in the observed increase of Izod impact strength in PP/EPDM/B-SiO<sub>2</sub> ternary composites with 20 wt% EPDM content. The schematic representation of toughening mechanism for PP/EPDM/SiO<sub>2</sub> composites is shown in Fig. 8. When EPDM content is 10 wt% (brittle region), the interparticle distance is very large. Although the addition of SiO<sub>2</sub> particles, at a certain degree, reduces the matrix–ligament thickness, the interparticle distance is too large to form the continuum percolation of stress volume around the EPDM particles, hence the yielding process cannot propagate and pervade over the PP matrix (seen in Fig. 8(a)). That is why the Izod impact strength of PP/EPDM/B-SiO<sub>2</sub> composites with 10 wt% EPDM content increases slightly with the addition of B-SiO<sub>2</sub> particles. When 20 wt% of EPDM are blended with 80 wt% of PP, the interparticle distance decreases sharply and becomes equivalent to the critical interparticle distance, so that the brittle–ductile transition occurs. After adding SiO<sub>2</sub> particles, EPDM particles are found to be closely surrounded by SiO<sub>2</sub> particles and a percolation of SiO<sub>2</sub> particles over the PP matrix is also observed. Thus the overlap of stress volume between EPDM and SiO<sub>2</sub> particles can be achieved since a large amount of SiO<sub>2</sub> particles agglomerate around EPDM particles and pervade over the PP matrix (seen in Fig. 8(b)). This is of great benefit to the percolation of the yielding process over the PP matrix, thus dramatically enhancing the Izod impact strength of the composite. However, for PP/EPDM binary composite with 30 wt% EPDM content, which is in the regions above the brittle–ductile transition (seen in Fig. 2(a)), the toughness becomes independent of EPDM content because of the mechanical saturation [25]. In other words, there is no need for SiO<sub>2</sub> particles to be the intermediate for the stress fields overlap between two rubber particles (seen in Fig. 8(c)). Therefore, the addition of SiO<sub>2</sub> particles does not have much effect on the Izod impact strength of PP/EPDM composite any longer. So, it is easy to understand the way that the core–shell phase structure obtained in PP/EPDM/A-SiO<sub>2</sub> composites, or

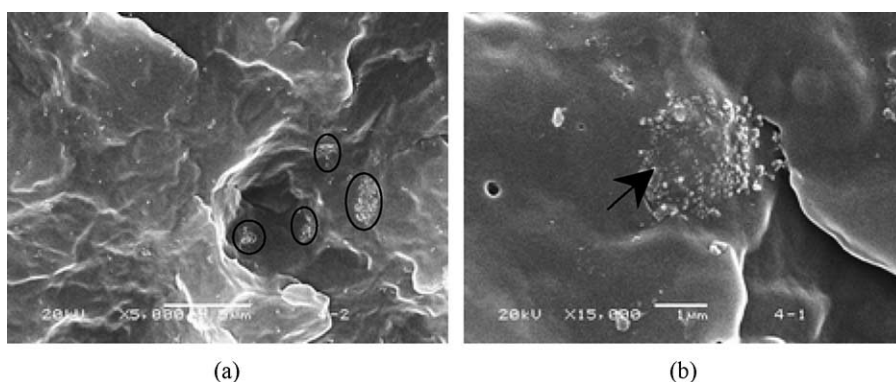


Fig. 7. SEM images of PP/B-SiO<sub>2</sub> binary blend under low (a) and high (b) magnifications (PP/B-SiO<sub>2</sub>=97:3).

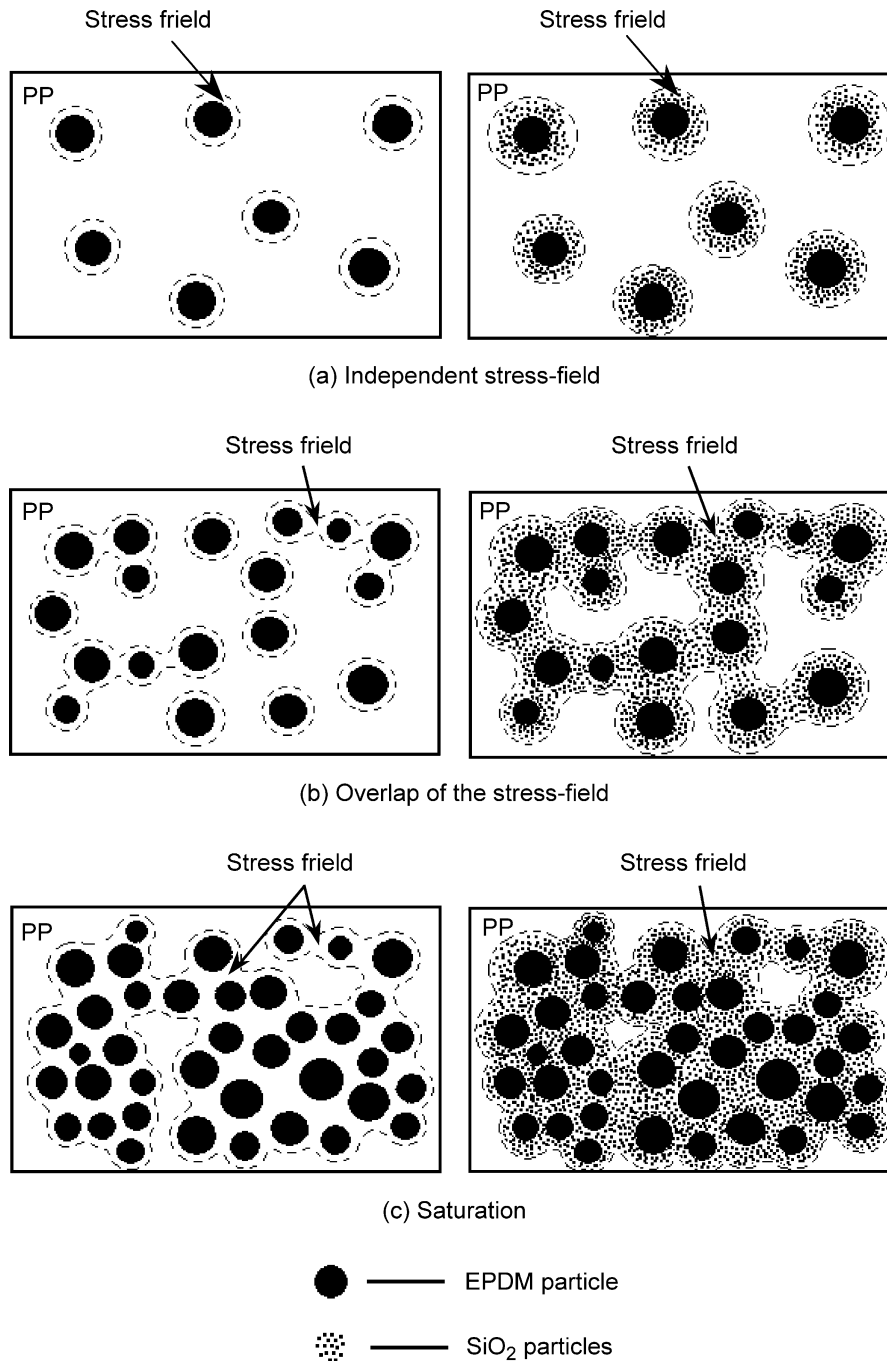


Fig. 8. The schematic representation of toughening mechanism for PP/EPDM/SiO<sub>2</sub> composites (a)  $\tau \gg \tau_c$ ; (b)  $\tau \approx \tau_c$ ; (c)  $\tau \ll \tau_c$ .

a separated dispersion structure with aggregated SiO<sub>2</sub> particles obtained in PP/EPDM/B-SiO<sub>2</sub> composites prepared by one-step processing method, cannot achieve a remarkable increase of Izod impact strength as shown in Fig. 3. For the core-shell phase structure with SiO<sub>2</sub> particles encapsulated by EPDM, just only a slight increase of the effective volume fraction of EPDM dispersed phases is achieved, which is of little avail to the improvement of Izod impact strength. For the separated dispersion structure with aggregated SiO<sub>2</sub> particles, large SiO<sub>2</sub> aggregates existing in PP matrix act as stress concentrations so that they cannot interact with the stress fields around EPDM particles effectively.

### 3.1.3. Impact-fractured surface of PP/EPDM/B-SiO<sub>2</sub> ternary composites

To gain more insight in understanding the toughening mechanism mentioned above, it is necessary to investigate the impact-fractured surface of PP/EPDM/B-SiO<sub>2</sub> composites with different EPDM content. Fig. 9 shows the impact-fractured surface of the selected samples, 90:10(90:10:5), 80:20(80:20:5), and 70:30(70:30:5) representing brittle, transition and ductile regions respectively. For PP/EPDM (90:10) binary composite and PP/EPDM/B-SiO<sub>2</sub> (90:10:5) ternary composite, the low Izod impact strengths ( $< 10 \text{ kJ/m}^2$ ) of them are clearly reflected by their impact-fracture surfaces.



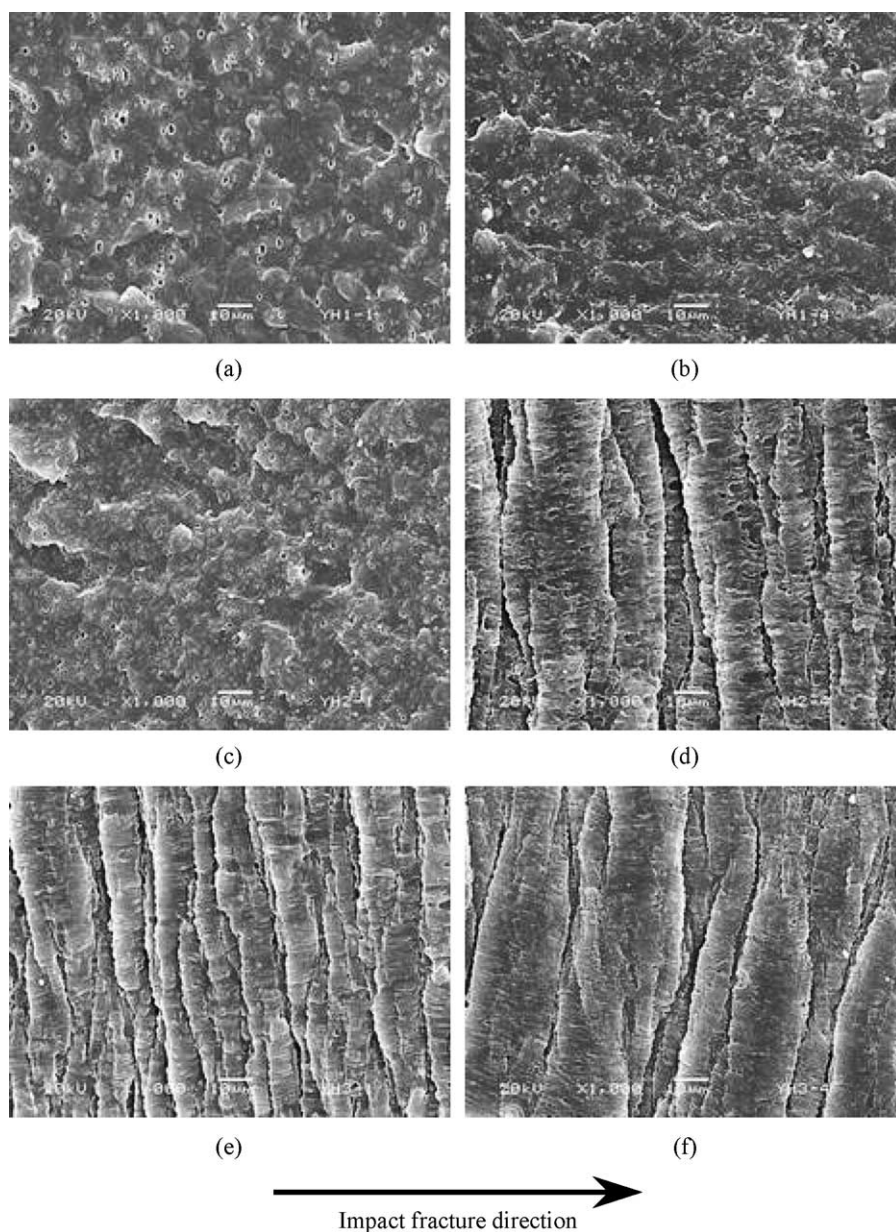


Fig. 9. SEM images of impact-fractured surface of PP/EPDM/B-SiO<sub>2</sub> composites PP/EPDM/B-SiO<sub>2</sub> (a) 90:10:0; (b) 90:10:5; (c) 80:20:0; (d) 80:20:5; (e) 70:30:0; (f) 70:30:5.

They reveal the typical morphology of a brittle failure; a relatively flat, smooth surface without any sign of deformation. The small, spherical holes seen in the fracture surface are probably due to the detachment of rubber or SiO<sub>2</sub> particles during the impact fracture (Fig. 9(a) and (b)). For PP/EPDM (80:20) binary composite, a smooth surface with many holes and some yielding sheets is seen (Fig. 9(c)), which suggests a relatively tough behavior. When adding 5 wt% B-SiO<sub>2</sub> particles, one observes many thick and long strips which are perpendicular to the impact fracture direction and are homogeneously distributed (Fig. 9(d)). The fracture process can be described as follows: when a ternary composite with such a microstructure, which is that SiO<sub>2</sub> particles aggregate around the EPDM particles and pervade over the PP matrix, is subjected to an impact loading, a large

number of crazes will form in the PP matrix at the beginning of the loading. However, the crazes will be effectively stopped once large amounts of (SiO<sub>2</sub> core)–(EPDM shell) structure are formed and SiO<sub>2</sub> particles pervade over the PP matrix. So the propagation of the crazes will be forced into the direction perpendicular to the impact fracture direction, which enables the sample to sustain a higher loading. This is probably attributed to the overlap of stress fields around rubber particles with that around SiO<sub>2</sub> particles. One observes not much difference of the impact-fractured surface between PP/EPDM (70:30) binary composite and PP/EPDM/SiO<sub>2</sub> (70:30:5) ternary composite (Fig. 9(e) and (f)), indicating that in this case there is no need for SiO<sub>2</sub> particles to be the intermediate for the stress fields overlap between two rubber particles.

#### 4. Conclusions

Using an appropriate processing method and adjusting the wettability of SiO<sub>2</sub> particles toward PP and EPDM, the phase structure of PP/EPDM/SiO<sub>2</sub> ternary composites can be successfully controlled. When hydrophilic SiO<sub>2</sub> particles (B-SiO<sub>2</sub>) are blended with PP/EPDM composite by using two-step processing method, a unique phase structure that EPDM particles are closely surrounded by B-SiO<sub>2</sub> particles is obtained. Meanwhile, the Izod impact strength PP/EPDM (80:20) blends dramatically increases by adding B-SiO<sub>2</sub> particles. The remarkable increase in the Izod impact strength can be tentatively attributed to the overlap of the stress volume between EPDM and SiO<sub>2</sub> particles due to the formation of the SiO<sub>2</sub>-surrounded EPDM particles. A more detailed work, including a calculation of the surface free energy, is needed to better understand the formation of the phase morphology and toughening mechanism.

#### Acknowledgements

We would like to express our great thanks to the National Natural Science Foundation of China (50533050, 20490220, 20574081 and 50290090) for Financial Support. This work was subsidized by the Special Funds for Major State Basic Research Projects of China (2003CB615600) and by Ministry of Education of China as a key project (104154).

#### References

- [1] Matonis VA, Small NC. *Polym Eng Sci* 1969;9:99.
- [2] Matonis VA, Small NC. *Polym Eng Sci* 1969;9:100.
- [3] Wen BY, Zhang XD, Li YC. *China Plast Ind* 2000;28(1):7.
- [4] Yu J, Wang SW, Huang GF. *Polym Mater Sci Eng* 2000;16(1):109.
- [5] Zhang XF, Zhang Y, Peng ZL. *J Appl Polym Sci* 2000;77:2641.
- [6] Percorini TJ, Hertzberg RW, Manson JA. *J Mater Sci* 1990;25:3385.
- [7] Kumar G, Neelakantan NR, Subramanian N. *Polym Plast Tech Eng* 1993;32:33.
- [8] Chang FC, Yang MY. *Polym Eng Sci* 1990;30:543.
- [9] Prephet K, Horanont P. *Polymer* 2000;41:9283.
- [10] Prephet K, Horanont P. *J Appl Polym Sci* 2000;76:1929.
- [11] Jancar J, Dibenedetto AT. *J Mater Sci* 1994;29:4651.
- [12] Cheng TW, Keskkula H, Paul DR. *Polymer* 1992;33:1606.
- [13] Merz EH, Claver GC, Baer M. *J Polym Sci* 1956;22:325.
- [14] Kunz-Douglass S, Beaumont WR, Ashby MF. *J Mater Sci* 1980;15:1109.
- [15] Yee AF. *J Mater Sci* 1977;12:757.
- [16] Maxwell MA, Yee AF. *Polym Eng Sci* 1981;21:205.
- [17] Bragaw GC. *Adv Chem Ser* 1971;99:86.
- [18] Bucknall CB. *Toughened plastics*. Appl Sci 1977. London.
- [19] Bucknall CB, Clayton D, Keast WE. *J Mater Sci* 1972;7:1443.
- [20] Bucknall CB, Drinkwater IC. *J Mater Sci* 1973;8:1800.
- [21] Newman S, Strella S. *J Appl Polym Sci* 1965;9:2297.
- [22] Wu S. *J Appl Polym Sci* 1990;30:73.
- [23] Wu S. *Polymer* 1985;26:1855.
- [24] Wu S. *J Appl Polym Sci* 1988;35:549.
- [25] Wu S. *Polymer* 1990;31:971.
- [26] Wu X, Zhu X, Qi ZN. *Eighth international conference on deformation, yield and fracture behavior of polymers*, Cambridge, UK; 1991. p. 78/1.
- [27] Zheng WG, Li Q, Qi ZN. *Chin Sci Bull* 1992;37:904.
- [28] Margolina A, Wu S. *Polymer* 1988;29:2170.
- [29] Zheng WG, Li Q, Qi ZN. *J Polym Eng* 1993;12:230.
- [30] Fu Q, Wang G. *Polym Int* 1993;30:309.